

Artificial neural network assisted optical spectroscopy as a prospective tool for prediction of blood glucose level

Ayyoob Jafari^{1,*}

¹ Biomedical Engineering Department, Islamic Azad University, Qazvin Branch, Qazvin, Iran

*corresponding author e-mail address: ajafari20@gmail.com

ABSTRACT

In the current work, the glucose level of human blood was examined within the range of 0-300 mg/dL and the optical absorbencies of obtained samples have been recorded in the wavelength range of 400-1100 nm. It was observed that the absorbance of blood is a function of glucose as well as hematocrit levels of blood. We determined a highly usable and optically transparent range of spectral absorbance for blood glucose level correlation assessment to be between 800-1000 nm. Then, 3-layer artificial neural network with back-propagation algorithm has been trained with some of experimental data to correlate the glucose level and absorbance spectra. The validity of trained network has also been checked with the train and test data. High validity of more 90% has been obtained in the case of the train and test data for prediction of glucose level. The results of this work are of usefulness in the design of new generation of non-invasive glucose monitoring systems by utilizing occlusion method.

Keywords *Glucose, Artificial Neural Network, optical spectroscopy, blood.*

1. INTRODUCTION

With worldwide spread of diabetes, self-monitoring of blood glucose get much attention in health care [1]. Currently the standard method (finger pricking) for the determination of patient's blood glucose level is invasive. Finger pricking method has some limitations such as the uncomfortableness of patients and the price of disposable glucometer sticks. There are many reports which introduce non-invasive methods for glucose determination, namely reverse iontophoresis [2], polarimetry [3], metabolic heat conformation [3], ultrasound [4], thermal emission [3], electromagnetic [3], photoacoustic [3], Infra-Red spectroscopy [5-11], Raman [12], light absorption [13] and impedance spectroscopy [14]. In spite of the high volume of conducted researches in this area, none of the reported methods has obtained enough accuracy to compete with invasive methods. One of the promising methods reported for non-invasive and continuous glucose monitoring is occlusion spectroscopy method [13]. In this method, a device (finger phantom) occludes blood flow in one of the fingers and then red/near-infrared (RNIR) light is passed through it. After that the amount of the passed light is measured with a detector. The intensity of the transmitted light could be correlated with the glucose level. With increasing the glucose level, the intensity of the transmitted light increases as light scattering decreases. In fact, glucose reduces the mismatch of refractive index between blood cells and their surrounding media which results in the decrease of scattering coefficient, and thus light could be transmitted via/with a shorter optical path [13]. For a practical measurement, it is necessary to find a relation between the intensity of transmitted light and glucose level. In order to be able to predict glucose level, OrSense Ltd. [13] utilized multiple (typically 10) wavelengths of light sources to obtain enough data. With the application of multiple light sources, the unwanted interferences caused by other blood parameters could be eliminated. Still the accuracy of occlusion method is not enough to

replace the standard method of glucose monitoring [3] and current researches are tackling this issue.

To correlate optical spectroscopy data with glucose level, it is necessary to apply a sophisticated algorithm which is capable of avoiding over fit and false correlations. On the other hand, artificial neural network (ANN) is an efficient tool to learn and predict sophisticated relationship of various experimental parameters [15,16]. The first step of an ANN utilization involves designing the network, then selecting the initial weights and biases, and finally using the best algorithm to change those during the learning process to find the best ones in order to produce desirable outputs from the input pattern [17]. Feed forward ANN with back-propagation training algorithm is one of the most established ANN algorithms for prediction purpose [17]. In this method, in every interval, current weights and biases are utilized for the computation of output from the input pattern and in the second step weights and biases are altered with a backward algorithm to justify the current output to the desired one.

There are many algorithms available for ANN training, such as gradient descent, conjugate gradient descent, quasi-Newton method, gradient descent with momentum, resilient back-propagation, variable learning rate back-propagation and Levenberg-Marquardt method. In all of these algorithms, an error function (usually sum square error (SSE) or mean square error (MSE)) is selected and then, the error function is minimized by changing the weights and biases step by step and numerically [16]. Among the aforementioned algorithms, Levenberg-Marquardt method is one of the most efficient and fastest algorithms of ANN training. In this method, the approximated Hessian matrix (second derivative) and Jacobean matrix are utilized to adjust the weights and biases (equation 1).

$$\mathbf{H} = \mathbf{J}^T \mathbf{J}, \mathbf{g} = \mathbf{J}^T \mathbf{e}, \mathbf{X}_{k+1} = \mathbf{X}_k - [\mathbf{H} + \mu \mathbf{I}]^{-1} \mathbf{g} \quad (1)$$

Here J is the Jacobean matrix containing the first derivatives of the network errors with respect to the weights and biases of ANN, X denotes weight or bias, g represents the gradient of the performance function, e is error (true output-network output), I holds for Identity Matrix, J^T is the transposed matrix of J , H denotes the Hessian matrix and the μ adopts a scalar value between 0 and 1 [16].

Due to the high learning potential of ANN for learning of the complex function, it usually make highly complex and unsmooth functions fit to the output data which in turn leads in overfitting problem. In over-fitted ANN, the error of training set is driven to a very small value but it becomes large when new data (test data) is given to the network [16].

One of the efficient ways to avoid over-fitting is to use lots of training data [16] which unfortunately increases the time and cost of experiments. Other possibilities for the avoidance of network generalization and over fit, are Model selection, Jittering, Early stopping, Weight decay, Bayesian learning [18], and Combining networks. In this work, a combination of Bayesian learning and Early-Stopping was used to avoid over-fitting problem. Bayesian learning resembles to Levenberg-Marquardt method and differs only in error function (equation 2) which contains new term consisting of the mean of the sum of squares of the network weights and biases [16].

$$EFBR = \gamma MSE + (1 - \gamma) MSE \quad (2)$$

In above equation, EFBR is the error function of Bayesian learning algorithm, γ denotes a parameter known as performance ratio which is calculated from weight and biases by statistical techniques, and MSE represents mean square error. By using this error function, smaller weights and biases have been obtained during the training which in turn led into smoother responses with lower over fit.

It is clear that by the application of optical spectrum consisting of a large number of data instead of an only limited number of light sources; the accuracy of occlusion spectroscopy method could be considerably heightened. Considering the development of mini-spectrophotometers, it can be predicted that these spectrophotometers will be available with a relatively lower price in future. Therefore it would be possible to use mini-spectrophotometers in upcoming non-invasive glucometers. Here, the optical spectra of blood samples with different glucose levels were recorded. Then the reliable part of the spectrum with high reliability and transparency was determined and selected to be correlated with the glucose level of the blood sample. Next applying artificial neural network, a relation between glucose level and optical absorbance has been obtained in the reliable part of the recorded spectra.

2. EXPERIMENTAL SECTION

The experiments were divided into several parts as follows: Data recording, neural network modeling, and testing of the obtained ANN model. For the first part, we examined the effects of glucose level and absorbance correlation. Then, the obtained data has been utilized to train the ANN in the second part. The trained ANN could be utilized to relate the glucose level with the optical spectra of blood. Finally, the trained ANN model has been checked and verified by applying the test data.

2.1. Data recording.

A blood packet of type B+ (the most common blood type in Iran [19]) was obtained from Iran blood bank center and its initial glucose and hematocrit levels were determined. As the optical transparency of the obtained blood samples was very high, it was diluted with distilled water 10 times so that the initial hematocrit level of 40% has been decreased to 4%. The initial glucose level was also determined by standard glucometer (Bionime) with disposable glucometer sticks of Rightest GS300. In the next step, various amounts of glucose (product of Merck Co., Germany) were added to the diluted blood samples to prepare various samples with different levels of glucose. The optical absorbencies of the prepared samples were recorded by PG80+ instrument in the wavelength range of 400-1100 nm. Table 1 shows the glucose level of the prepared samples.

Table 1. Glucose level of prepared samples

Sample	glycemia	Glucose Level (mg/dl)	Glucose Level (mmol/l)
1	Hypoglycemia	3.2	0.16
2	Hypoglycemia	6.3	0.32

Sample	glycemia	Glucose Level (mg/dl)	Glucose Level (mmol/l)
3	Hypoglycemia	11.8	0.60
4	Hypoglycemia	16.7	0.84
5	Hypoglycemia	26.8	1.35 (*)
6	Hypoglycemia	34.8	1.76
7	Hypoglycemia	42.2	2.13
8	Hypoglycemia	59.1	2.98
9	Normal	71.2	3.59
10	Normal	85.7	4.32 (*)
11	Normal	100	5.05
12	Hyperglycemia	124	6.26
13	Hyperglycemia	151	7.62
14	Hyperglycemia	185	9.34
15	Hyperglycemia	211	10.65 (*)
16	Hyperglycemia	248	12.51
17	Hyperglycemia	270	13.62
18	Hyperglycemia	298	15.04

2.2. Neural network modeling.

The data was gathered in order to acquire sufficient input data to train, validate and test the ANN. Three-layered feed forward ANN was employed for the training and 3, 20 and 1 neuron(s) were utilized in the first, hidden and output layers, respectively. The input pattern consists of glucose level as well as wavelength and the output data consisted of absorbance (Fig. 1).

Tan-sigmoid (tansig) function (equation 3) was selected as the transfer function of the first and hidden layers, while a linear function was selected for the output layer transfer function. The ANN modeling was conducted using the Matlab software.

$$\text{Tansig}(N) = [2/(1 + e^{-2N})] - 1 \quad (3)$$

Before the training, validating and testing the designed ANN, all of the input data was preprocessed and converted into values in the range of 0 to 1 to improve the generalization of the

network. In order to inhibit the over-fitting problem, Bayesian regularization training method combined with early stopping was applied therein.

2.3. Testing the obtained ANN model.

The spectra with the glucose levels of 26.8, 85.7 and 211 mg/dL were utilized as the test data to assess the integrity of the trained network in different glucose levels (low, medium and high levels).

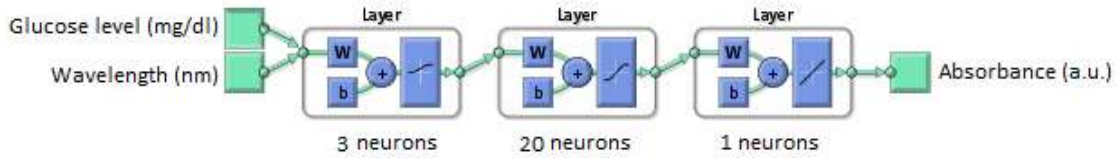


Figure 1. Neural Network topology.

3. RESULTS SECTION

The recorded absorbencies of the prepared samples with different amounts of glucose have been depicted in Fig. 2. The results clearly showed that absorbance has been decreased by increasing glucose level. These results are in agreement with the aforementioned mechanism in which the glucose reduces the refractive index of the mismatch of blood cells and their surrounding media and thus reduces scattering. The peaks observed in the wavelength range of 400-650 nm are mainly related to the absorbance of red blood cells (hemoglobin). The changes of absorbance with glucose level are higher in the wavelength ranges of 700 to 1000 nm. The absorbance decreased as the wavelength increased in this range. Fig. 3 also shows that with the decrease of the hematocrit level from 4% to 2%, the absorbance of blood has also been decreased. This figure also shows that in different levels of hematocrit (2%) the absorbance is still a function of glucose level, but that the influence of glucose level on absorbance spectra was weakened as the changes were very small when the glucose level changed from 100 mg/dl to 294 mg/dl.

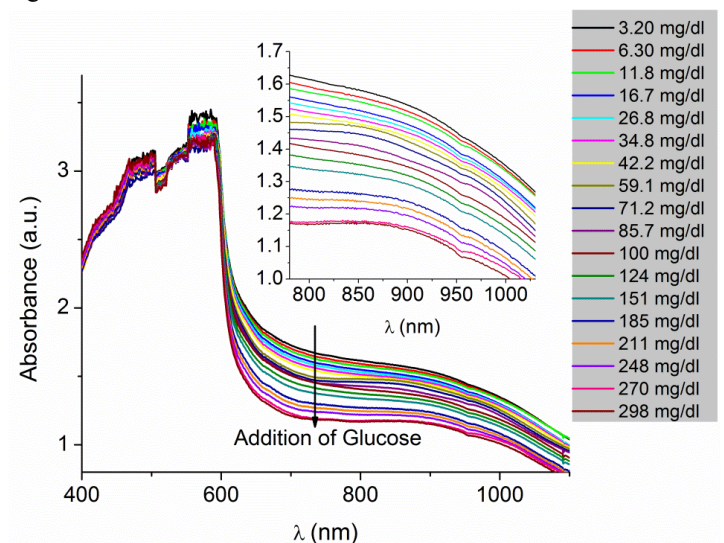


Figure 2. Optical absorbance spectra of blood samples with different amounts of glucose.

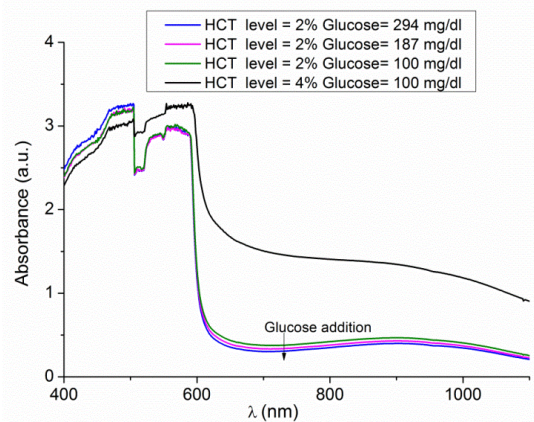


Figure 3. Effect of hematocrit (HCT) level on the optical absorbance spectra of blood.

Figure 4 shows the prediction of the absorbance spectra of glucose level of 26.9 mg/dL with the trained ANN when the whole spectra of the samples within the range of 400-1100 nm were utilized for the ANN training. Although the predicted and recorded spectra are almost fitted together, some differences could be especially seen in the wavelength range of 400-650 nm. These small differences are enough to deteriorate the accuracy of prediction and increase the uncertainty of predicted values.

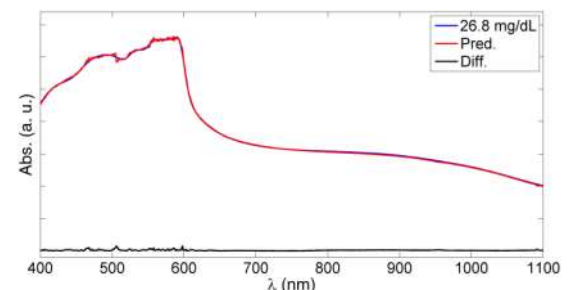


Figure 4. Prediction of whole absorbance spectra of blood sample with glucose level of 26.9 mg/dl by the trained ANN (Differences of prediction and recorded spectra have also be shown in this figure).

In the next step, to increase the accuracy of the prediction and also to similarize the spectra with normal occlusion

spectroscopy tests, a limited part of the absorbance spectra has been selected. Two criteria were considered for the selection. Firstly, the absorbance of blood should not be high to let enough light pass through it, and second the reliability and repeatability of spectra should be sufficiently high. Fig. 5 shows the repeated record of the spectra for one of the samples. The differences of this absorbance are also showed in this figure. It is observed that the differences are too small in the range of 800-1000 nm. Therefore, the wavelength range of 800-1000 nm is suitable for an occlusion spectroscopy test. The recorded spectra of the training sample in this range have been utilized to train the ANN.

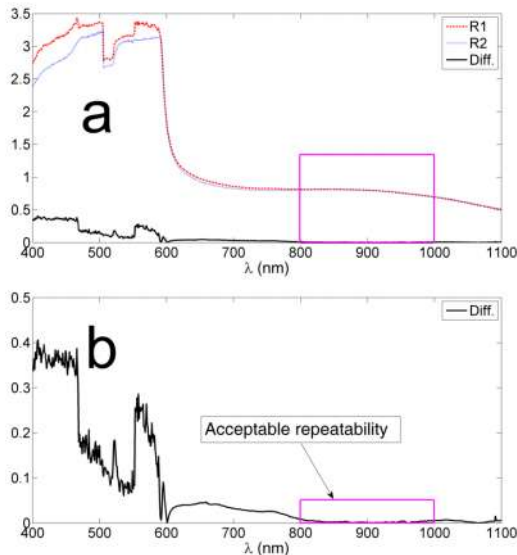


Figure 5. a) Two absorbance spectra related to one sample and their differences b) the magnification of the differences of two recorded spectra.

Fig. 6 shows the reduction of the performance function during the ANN learning. As figure demonstrates, the training was stopped in the iteration of 1020. Here we deliberately stopped the further training to inhibit over fitting (early stopping is one of the efficient methods to inhibit over-fitting)

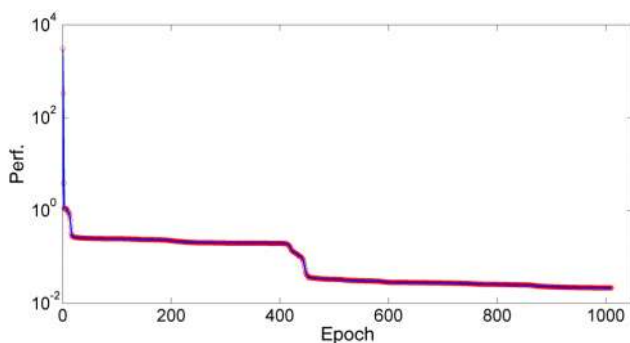


Figure 6. Reduction of performance function vs. learning iteration (epoch).

Fig. 7a shows the prediction of absorbance spectra in the wavelength range of 800-1000 nm for the sample containing 34.8 mg/dl of glucose. The differences of the prediction and recorded spectra are shown in this figure as well as Fig. 7b. It can be seen that differences are negligible (<0.01) in the investigated wavelength range and that the differences are not a function of wavelength. This result indicates highly accurate prediction of ANN in case of train data.

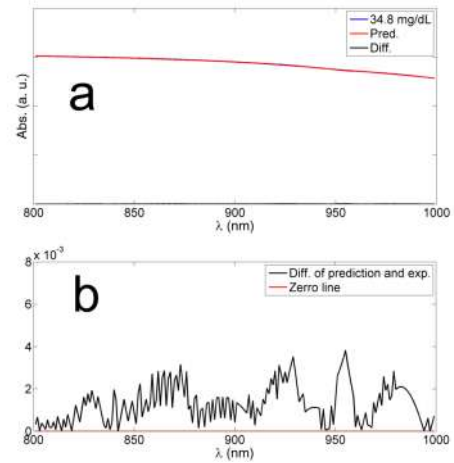


Figure 7. a) Recorded and prediction absorbance spectra of blood sample with glucose level of 34.8 mg/dl by the trained ANN in the wavelength range of 800-1000 nm b) Magnified difference curve of prediction and experimentally recorded spectra.

To find glucose level of test sample with the designed topology of ANN, the absorbance is predicted for different glucose levels and the sum of the squared error (SSE) of the differences of prediction and experimental spectrum (for test sample) is calculated for all glucose levels. The glucose level associated with the minimum of SSE will be the predicted glucose value for test sample. As mentioned in table 1, the samples with the glucose levels of 26.8, 85.7 and 211 mg/dL were utilized as the test data. Fig. 8 shows the SSE for different glucose levels during the prediction by the described algorithm. It exhibits that the SSE was minimized at the glucose levels of 25, 83, 227 mg/dL for test samples which are very close to their actual values of 26.8, 85.7 and 211 mg/dL, respectively (accuracy of more than 90%).

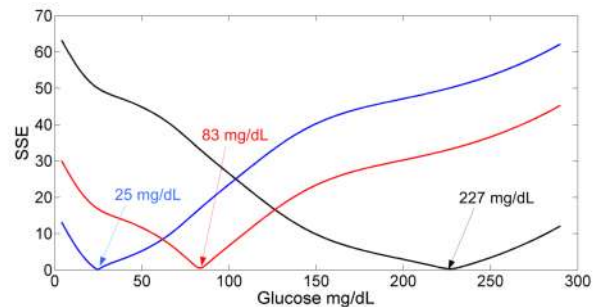


Figure 8. Minimization of SSE to find glucose levels of test samples with actual glucose values of 26.8, 85.7 and 211 mg/dL.

The current work is an introduction for future researches and many other parameters could be added as the input or output parameters of ANN in order to increase the accuracy and functionalities of ANN prediction. For example, hematocrit level as well as the color of skin, blood type and a calibration coefficient (which is the characteristic of each person and is determined by comparison of initial prediction of this method with the standard method) could be added as input parameters. The topology of ANN can also be modified to predict the oxygen saturation of blood.

4. CONCLUSIONS

In sum, the results of the optical spectroscopy of the blood samples showed that the glucose and hematocrit levels of blood affect the absorbance of blood samples. Strictly speaking, with increasing the glucose level, the absorbance decreased while with increasing the hematocrit level, the absorbance increased. The highly reliable part of the optical spectra of blood sample with the desired transparency has also been found to be in the range of 800-

1000 nm. Then with the application of a three layer artificial neural network which was trained by a Bayesian regularization algorithm, the glucose levels of blood were correlated with the absorbance spectra of the blood samples. The trained ANN could predict the glucose level of the test sample with accuracy of more than 90%.

5. REFERENCES

- [1] Vashist S.K., Zheng D., Al-Rubeaan K., Luong J.H.T., Sheu F.-S., Technology behind commercial devices for blood glucose monitoring in diabetes management: A review, *Analytica Chimica Acta* 703, 124-136, **2011**
- [2] McCormick C., Heath D., Connolly P., Towards blood free measurement of glucose and potassium in humans using reverse iontophoresis, *Sensors and Actuators B*, 166-167, 593-600, **2012**
- [3] Amaral C.E.F.d., Wolf B., Current development in non-invasive glucose monitoring, *Medical Engineering & Physics*, 30, 541-549, **2008**
- [4] Chen C.-S., Wang K.-K., Jan M.-Y., Hsu W.-C., Li S.-P., Wang-Lin Y.-Y., Bau J.-G., Noninvasive blood glucose monitoring using the optical signal of pulsatile microcirculation: a pilot study in subjects with diabetes, *Journal of Diabetes and Its Complications*, 22, 371-376, **2008**
- [5] Ding Q., Small G.W., Arnold M.A., Evaluation of nonlinear model building strategies for the determination of glucose in biological matrices by near-infrared spectroscopy, *Analytica Chimica Acta*, 384, 333-343, **1999**
- [6] Kasemsumran S., Du Y.P., Maruo K., Ozaki Y., Improvement of partial least squares models for in vitro and in vivo glucose quantifications by using near-infrared spectroscopy and searching combination moving window partial least squares, *Chemometrics and Intelligent Laboratory Systems*, 82, 97 - 103, **2006**
- [7] Pleitez M., Lilienfeld-Toal H.v., Mäntele W., infrared spectroscopic analysis of human interstitial fluid in vitro and in vivo using FT-IR spectroscopy and pulsed quantum cascade lasers (QCL): Establishing a new approach to non invasive glucose measurement, *Spectrochimica Acta Part A*, 85, 61-65, **2012**
- [8] Saiga N., Hamada C., Ikeda J., Near infrared spectroscopy assessment of the glucose solution processed by ultrasonic cavitation, *Ultrasonics*, 44, Supplement, 0, e101-e104, **2006**
- [9] Xu K., Qiu Q., Jiang J., Yang X., Non-invasive glucose sensing with near-infrared spectroscopy enhanced by optical measurement conditions reproduction technique, *Optics and Lasers in Engineering*, 43, 1096-1106, **2005**
- [10] Sun M., Chen N., Non-invasive measurement of blood glucose level by time-resolved transmission spectroscopy: A feasibility study, *Optics Communications*, 285, 1608-1612, **2012**
- [11] Li Q.-B., Li L.-N., Zhang G.-J., A nonlinear model for calibration of blood glucose noninvasive measurement using near infrared spectroscopy, *Infrared Physics & Technology* 53, 410-417, **2010**
- [12] Shih W.-C., Bechtel K.L., Feld M.S., *Non-invasive Glucose Sensing with Raman Spectroscopy* Massachusetts Institute of Technology, Cambridge, MA 02139, **2007**
- [13] Amir O., Weinstein D., Zilberman S., Less M., Perl-Treves D., Primack H., Weinstein A., Gabis E., Fikhte B., Karasik A., Continuous Noninvasive Glucose Monitoring Technology Based on "Occlusion Spectroscopy", *Journal of Diabetes Science and Technology*, 1, 463-469, **2007**
- [14] Caduff A., Dewarrat F., Talary M., Stalder G., Heinemann L., Feldman Y., Non-invasive glucose monitoring in patients with diabetes: A novel system based on impedance spectroscopy, *Biosensors and Bioelectronics*, 22, 598-604, **2006**
- [15] Kamaloo A., Ganjkanlou Y., Aboutalebi S.H., Nouranian H., Modeling of compressive strength of metakaolin based geopolymers by the use of artificial neural network, *International Journal of Engineering*, 23, 2, 145-152, **2010**
- [16] Pazouki M., Ganjkanlou Y., Tofigh A.A., Hosseini M.R., Aghaie E., Ranjbar M., Optimizing of Iron Bioleaching from a Contaminated Kaolin Clay by the Use of Artificial Neural Network, *International Journal of Engineering*, 25, 2, 81-87, **2012**
- [17] Hagan M.T., Demuth H.B., Beale M.H., *Neural network design*. PWS Publishing, Boston. **1996**
- [18] MacKay D.J.C., *Bayesian methods for adaptive models*, California Institute of Technology, Pasadena, California, **1992**
- [19] Abouzari M., Behzadi M., Rashidi A., Low frequency of blood group A in secondary central nervous system lymphoma, *Surg Neurol Int*, 3, 95-97, **2012**.

6. ACKNOWLEDGEMENTS

Authors gratefully acknowledge the financial support by the Islamic Azad University, Qazvin Branch within the research project.

© 2016 by the authors. This article is an open access article distributed under the terms and conditions of the Creative Commons Attribution license (<http://creativecommons.org/licenses/by/4.0/>).